Ministry of Science and Higher Education
Republic of Poland

JAGIELLONIAN UNIVERSITY IN KRAKÓW

EUROPEAN SPACE AGENCY

15 - 19 June 2026 | Auditorium Maximum of the Jagiellonian University, Kraków, Poland

FRINGE 2026

Assessment of Season-Dependent Sentinel-1 SAR Coherence Reliability in Freeze-Thaw Dominated Terrain: A Longyearbyen Case Study

Jmukhadze Marisha, Bheesetty Puneeth
Warsaw University of Technology

Challenges for InSAR Reliability in Arctic Terrain

- Freeze-thaw cycles alter radar scattering properties
- Snow accumulation and snowmelt reduce coherence
- Surface moisture causes temporal decorrelation
- Low coherence decreases confidence in InSAR analysis

Reliable InSAR monitoring depends on maintaining sufficient coherence between image acquisitions

Study Area: Longyearbyen, Svalbard

- Continuous permafrost and seasonal snow cover
- Strong freeze-thaw transitions throughout the year
- Diverse terrain includes snow, exposed ground, water, and permafrost features
- Rapid environmental changes affect radar coherence
- Ideal testbed where InSAR conditions range from highly stable to highly decorrelated
- Long Sentinel-1 archive enables multi-season and multi-year analysis

Extreme environmental conditions make Longyearbyen a natural laboratory for assessing InSAR reliability.

Research Objective

Sentinel-1 SAR Images

Coherence Maps

Reliability Assessment

Seasonal Comparison

Data and Methodology

Parameter	Value
Mission	Sentinel-1
Product Type	SLC- 1A/1B
Acquisition Mode	IW
Orbit	Ascending
Polarization	HH
Study Area	Longyearbyen, Svalbard
Time Period	2019-2021

Coherence Processing Workflow

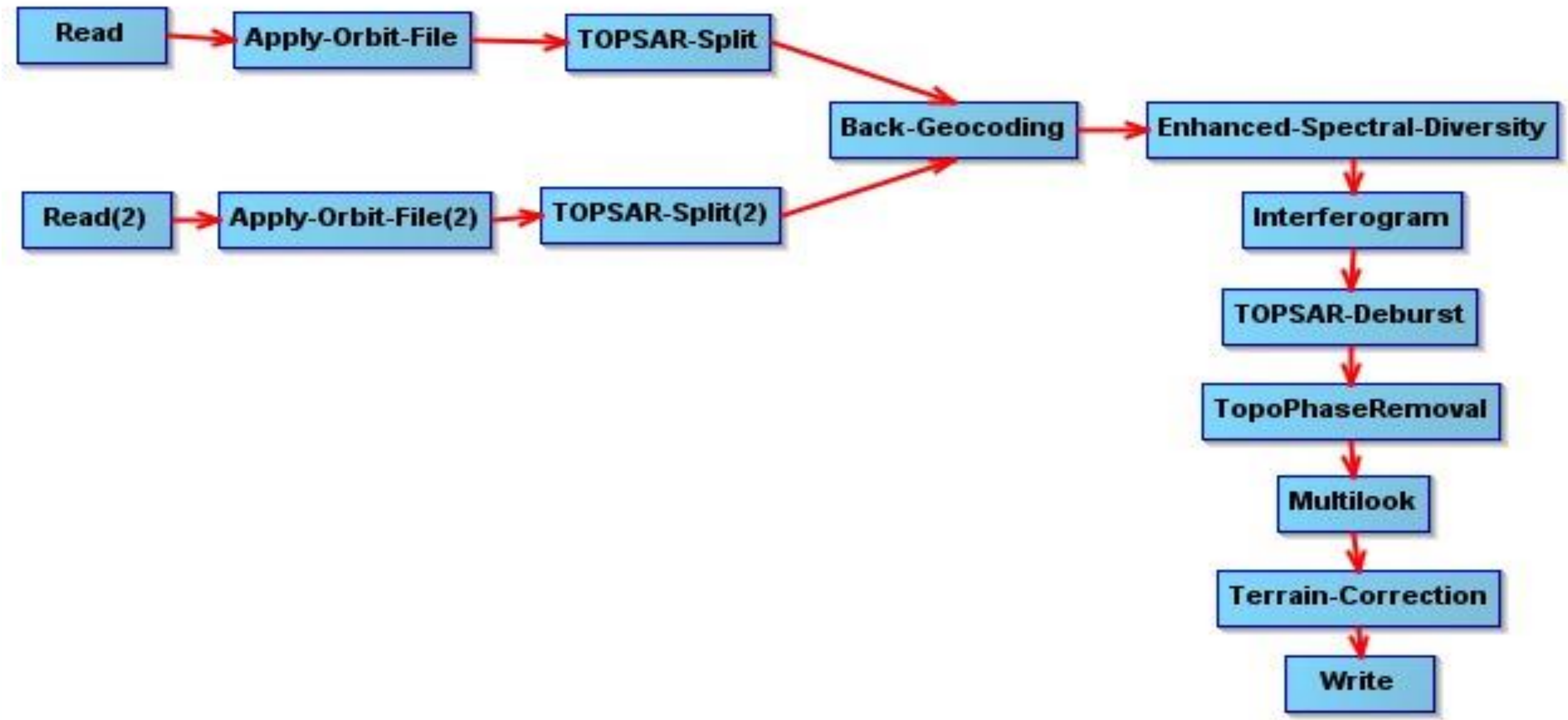

Zero-masked coherence overview

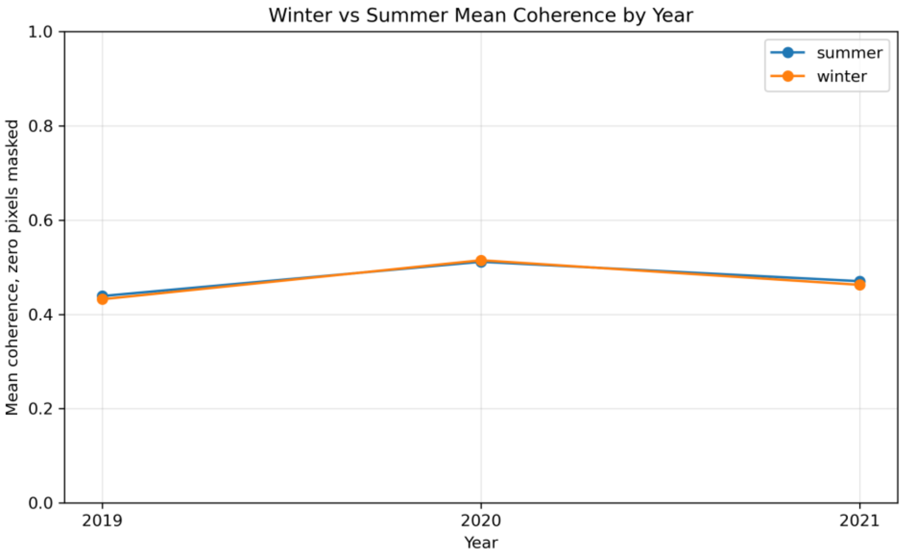

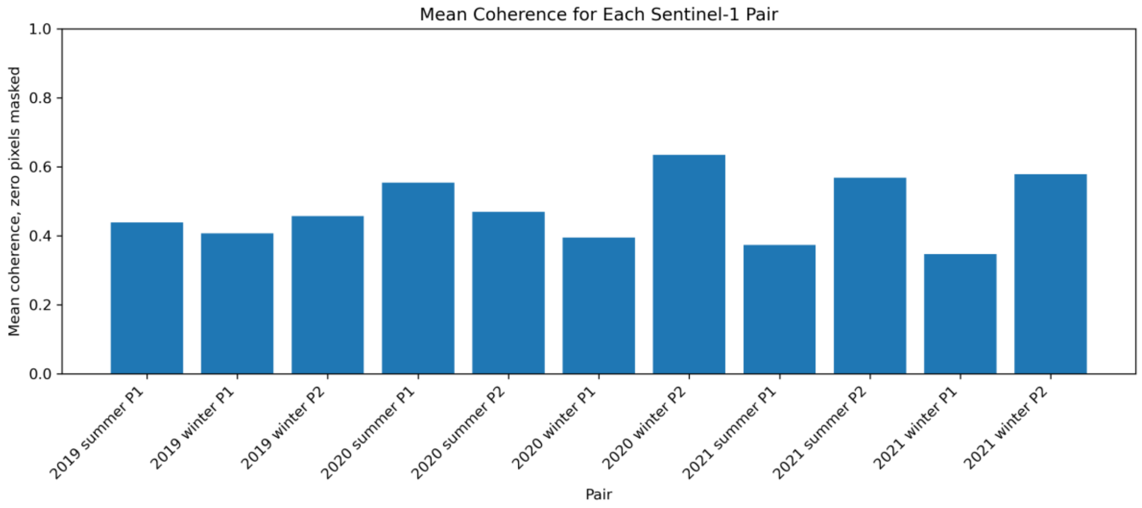

Year	Pairs	Mean	Median	Std dev	Reliable >0.5	Zero masked
2019	3	0.434	0.399	0.025	36.6%	88.4%
2020	4	0.513	0.523	0.104	52.3%	87.4%
2021	4	0.466	0.470	0.124	42.3%	82.4%

Statistic basis: coherence > 0 and <= 1; zero/near-zero pixels masked before statistics.

Annual readout
- Highest annual coherence: 2020 (mean 0.513, reliable pixels 52.3%).
- Lowest annual coherence: 2019 (mean 0.434).

Why coherence fluctuates between winter and summer

Frozen / stable

Frozen ground can preserve stable scatterers and reduce short-term moisture changes. When that stability dominates, histograms shift toward higher coherence and maps show more green/yellow areas.

Thaw / wet

Active thaw, meltwater, wet snow, and changing surface roughness can decorrelate the radar signal. The measured seasonal result is therefore year- and pair-specific, not a fixed winter/summer rule.

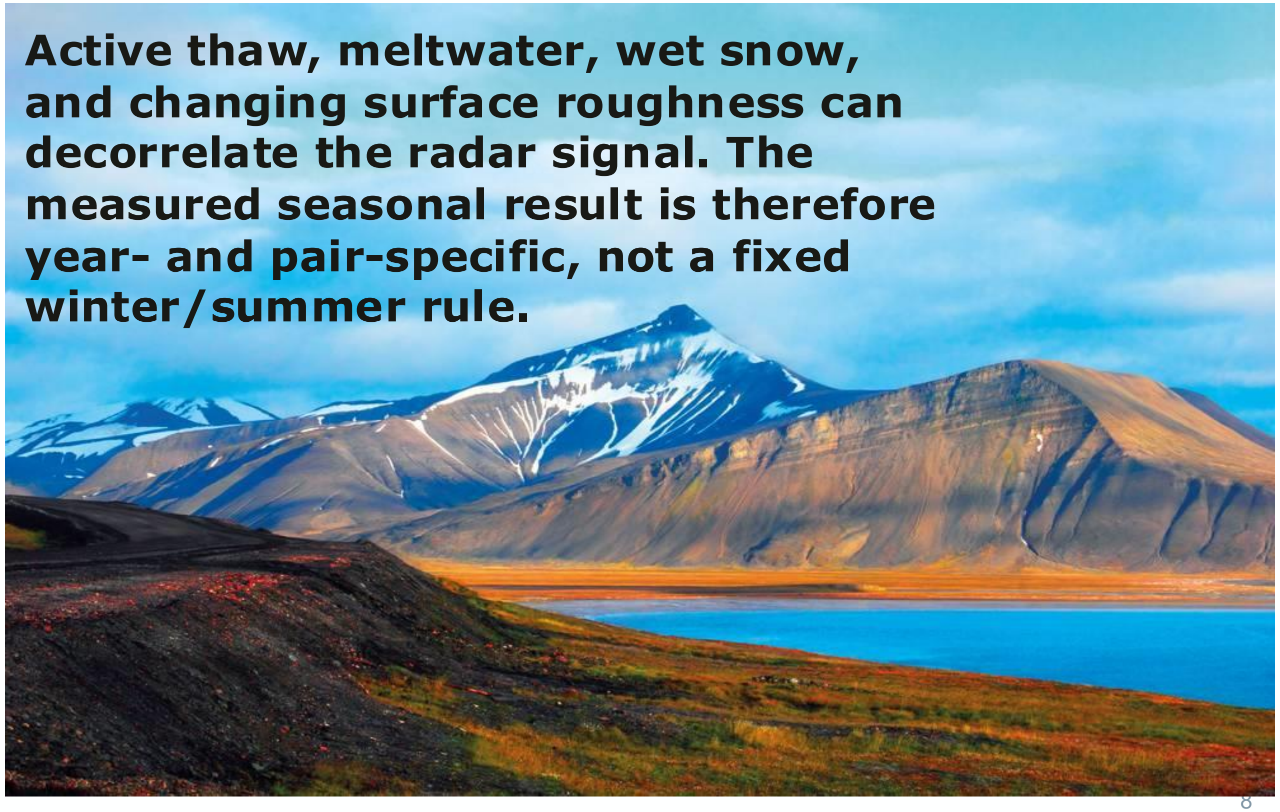

All sample pairs and acquisition dates

All acquisitions use a 6-day temporal baseline; mean coherence shown for quick reference.

Year	Season	Pair	Master date	Slave date	Days	Mean coh.
2019	Winter	1	2019-01-01	2019-01-07	6	0.407
2019	Winter	2	2019-01-25	2019-01-31	6	0.457
2019	Summer	1	2019-06-30	2019-07-06	6	0.439
2020	Winter	1	2020-01-02	2020-01-08	6	0.394
2020	Winter	2	2020-01-26	2020-02-01	6	0.635
2020	Summer	1	2020-06-30	2020-07-06	6	0.554
2020	Summer	2	2020-07-24	2020-07-30	6	0.469
2021	Winter	1	2021-01-02	2021-01-08	6	0.346
2021	Winter	2	2021-01-26	2021-02-01	6	0.579
2021	Summer	1	2021-07-01	2021-07-07	6	0.373
2021	Summer	2	2021-07-25	2021-07-31	6	0.568

Mean, median, and standard deviation of coherence

Year-season	Pairs	Mean	Median	Std dev	Reliable >0.5	Low <0.3
2019 Winter	2	0.432	0.405	0.035	35.9%	31.8%
2019 Summer	1	0.439	0.387	-	37.9%	36.8%
2020 Winter	2	0.515	0.518	0.170	52.3%	20.7%
2020 Summer	2	0.511	0.529	0.060	52.3%	25.2%
2021 Winter	2	0.463	0.460	0.164	41.4%	30.7%
2021 Summer	2	0.470	0.479	0.138	43.2%	32.1%

Important results
- Best pair: 2020 Winter pair 2 (2020-01-26 to 2020-02-01), mean 0.635.
- Largest season-level fluctuation between pairs: 2020 Winter (std dev 0.170).
- 2020 is the most reliable annual set; 2019 is the weakest annual set in the zero-masked summaries.

Std dev is between-pair standard deviation for each year-season; a single-pair season is shown as '-'.

Coherance heatmaps

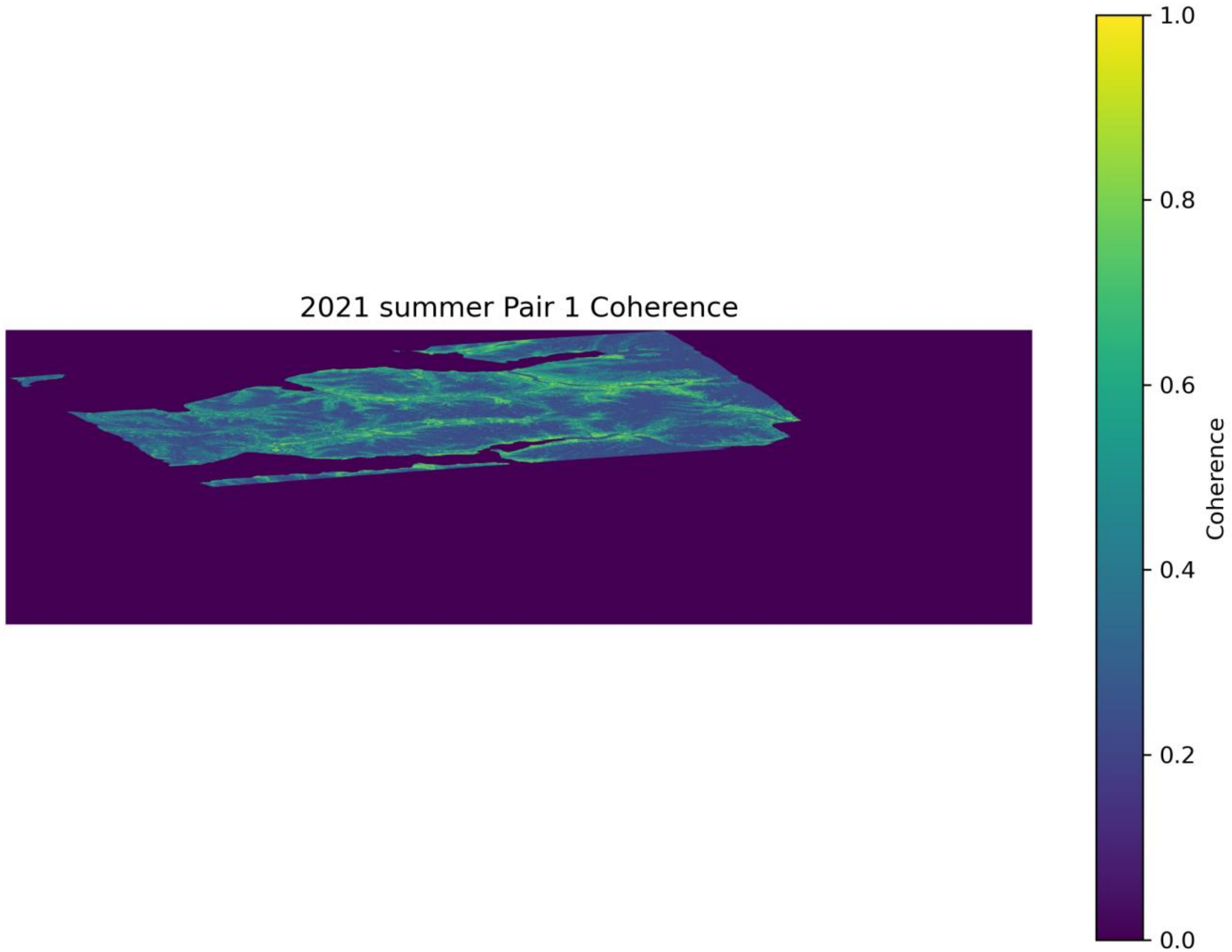

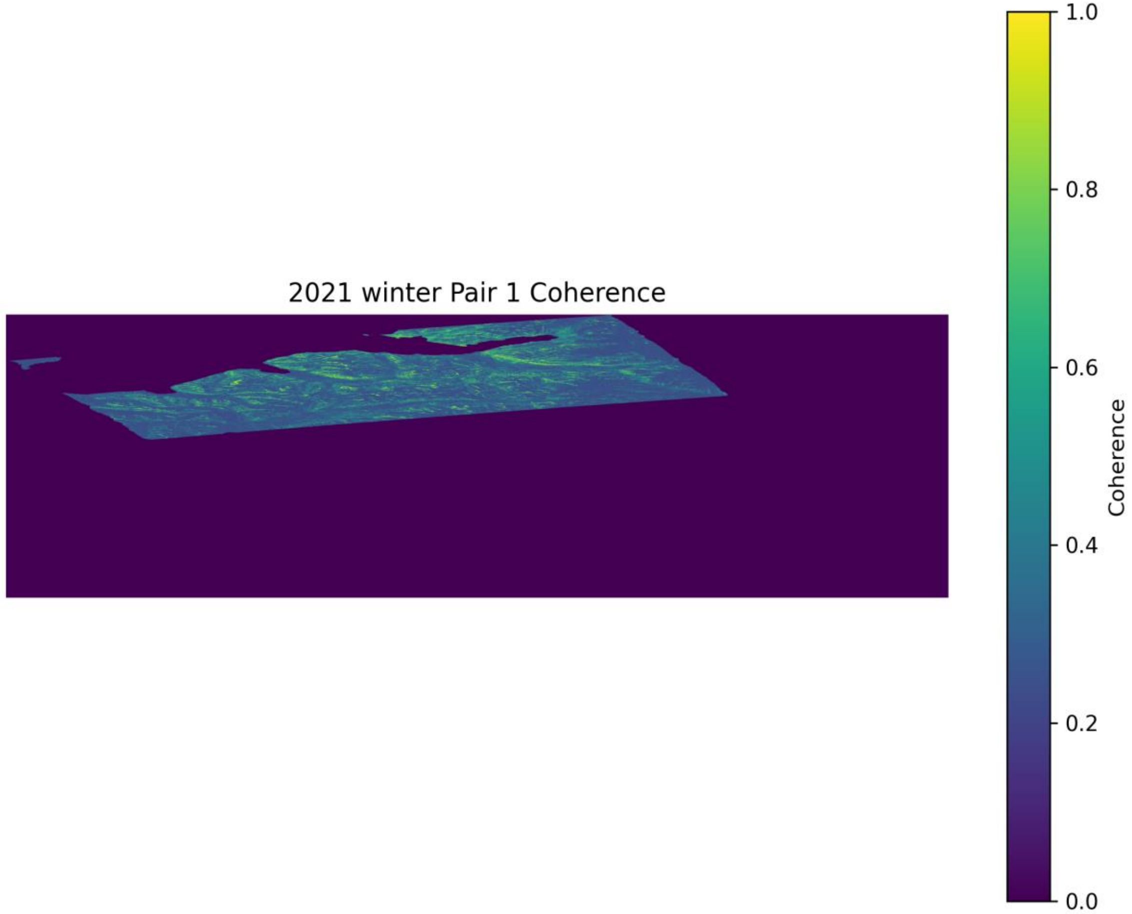

Summer coherence heatmaps

5 pairs | mean range 0.373-0.568 | best: 2021 P2 (0.568) | lowest: 2021 P1 (0.373)

2019 P1 2019-06-30 to 2019-07-06 mean 0.439

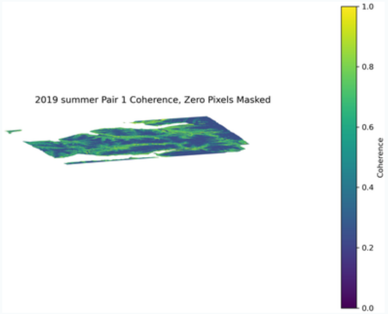

2020 P1 2020-06-30 to 2020-07-06 mean 0.554

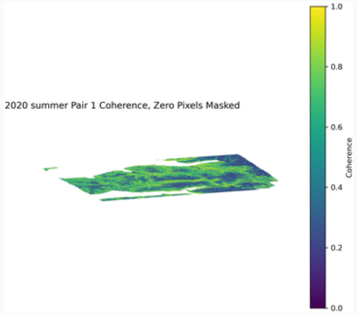

2020 P2 2020-07-24 to 2020-07-30 mean 0.469

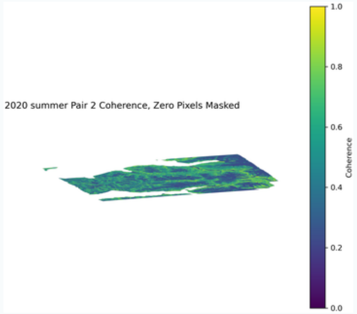

2021 P1 2021-07-01 to 2021-07-07 mean 0.373

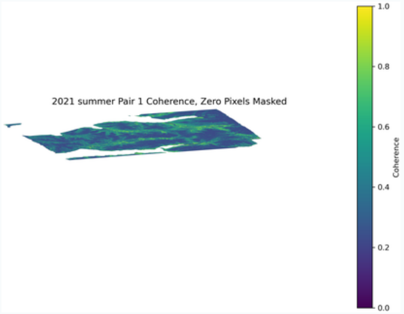

2021 P2 2021-07-25 to 2021-07-31 mean 0.568

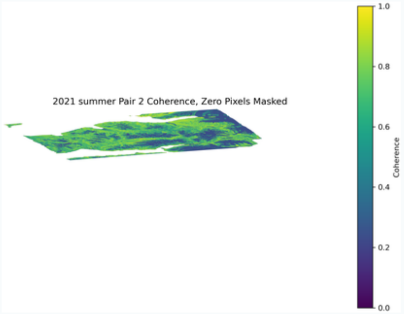

Across summer acquisitions, coherence varies from 0.373 to 0.568. The strongest pair is 2021 pair 2 (2021-07-25 to 2021-07-31), while the lowest is 2021 pair 1. Reliable-pixel share averages 45.8% and low-coherence pixels average 30.3% among non-zero pixels.
Map brightness/green-yellow areas indicate higher coherence; darker blue/purple zones mark less reliable scatterers.

Winter coherence heatmaps

6 pairs | mean range 0.346-0.635 | best: 2020 P2 (0.635) | lowest: 2021 P1 (0.346)

2019 P1 2019-01-01 to 2019-01-07 mean 0.407

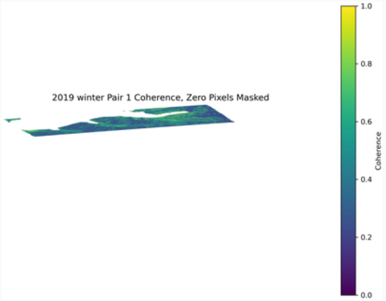

2019 P2 2019-01-25 to 2019-01-31 mean 0.457

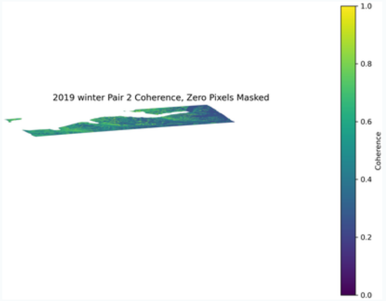

2020 P1 2020-01-02 to 2020-01-08 mean 0.394

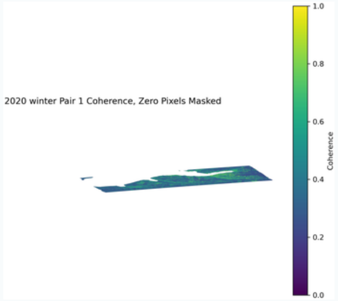

2020 P2 2020-01-26 to 2020-02-01 mean 0.635

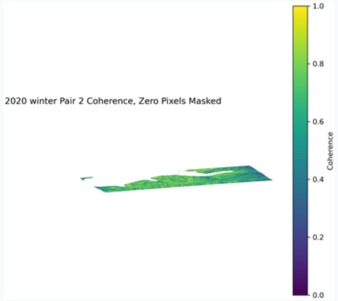

2021 P1 2021-01-02 to 2021-01-08 mean 0.346

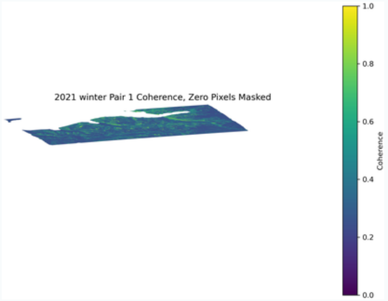

2021 P2 2021-01-26 to 2021-02-01 mean 0.579

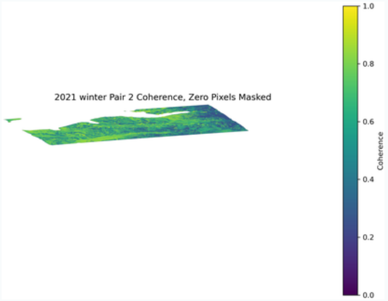

Across winter acquisitions, coherence varies from 0.346 to 0.635. The strongest pair is 2020 pair 2 (2020-01-26 to 2020-02-01), while the lowest is 2021 pair 1. Reliable-pixel share averages 43.2% and low-coherence pixels average 27.7% among non-zero pixels. Map brightness/green-yellow areas indicate higher coherence; darker blue/purple zones mark less reliable scatterers.

Summer coherence histograms

5 pairs | mean range 0.373-0.568 | best: 2021 P2 (0.568) | lowest: 2021 P1 (0.373)

2019 P1 2019-06-30 to 2019-07-06 mean 0.439

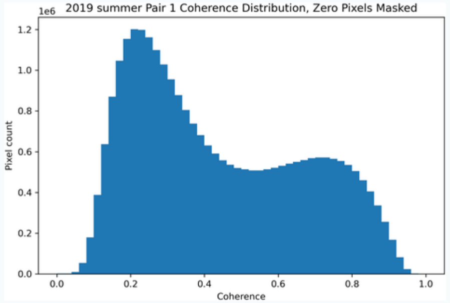

2020 P1 2020-06-30 to 2020-07-06 mean 0.554

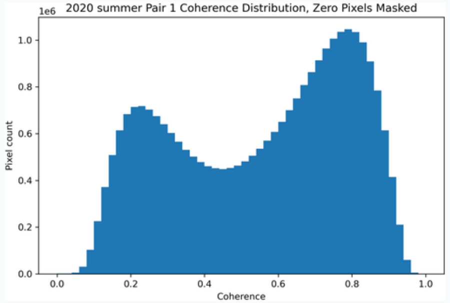

2020 P2 2020-07-24 to 2020-07-30 mean 0.469

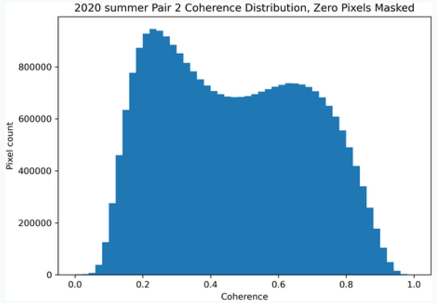

2021 P1 2021-07-01 to 2021-07-07 mean 0.373

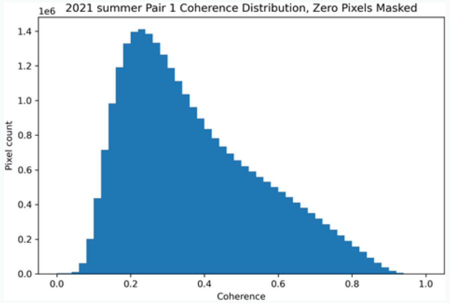

2021 P2 2021-07-25 to 2021-07-31 mean 0.568

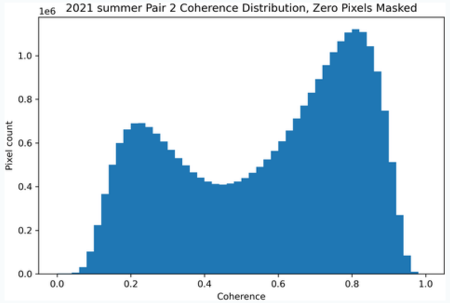

A distribution shifted toward higher values indicates a greater proportion of stable scatterers.
The summer histograms show noticeable variability among acquisitions, reflecting differences in moisture conditions, snowmelt, and surface state throughout the thaw season.
These distributions help visualize how coherence is distributed across the entire study area rather than relying only on mean values.

Winter coherence histograms

6 pairs | mean range 0.346-0.635 | best: 2020 P2 (0.635) | lowest: 2021 P1 (0.346)

2019 P1 2019-01-01 to 2019-01-07 mean 0.407

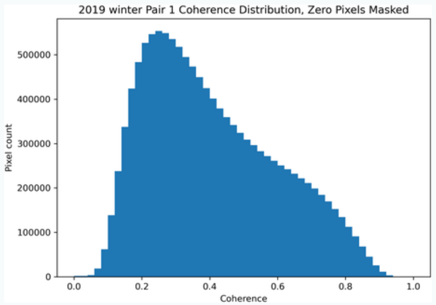

2019 P2 2019-01-25 to 2019-01-31 mean 0.457

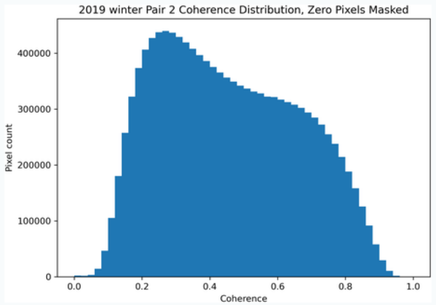

2020 P1 2020-01-02 to 2020-01-08 mean 0.394

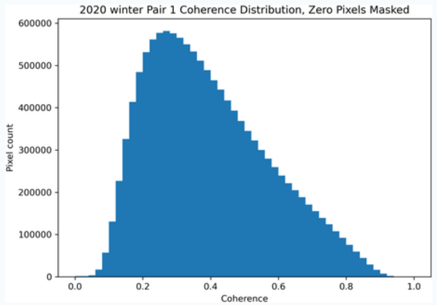

2020 P2 2020-01-26 to 2020-02-01 mean 0.635

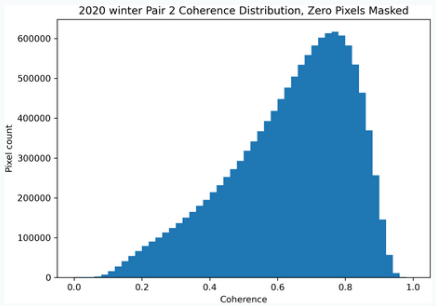

2021 P1 2021-01-02 to 2021-01-08 mean 0.346

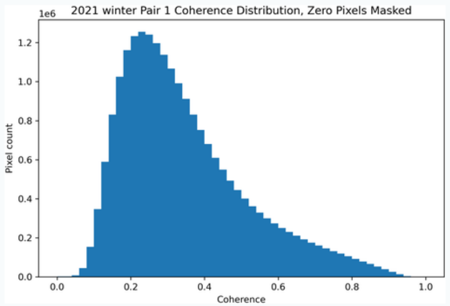

2021 P2 2021-01-26 to 2021-02-01 mean 0.579

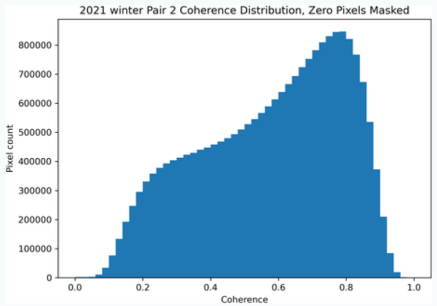

The winter histograms generally exhibit stronger concentrations of higher coherence values. Several winter acquisitions show distributions shifted toward more stable coherence levels compared with the summer cases.

- **After both summer and winter histograms:**

-

Summer histograms are more mixed and often bimodal, meaning part of the terrain remains coherent while other areas decorrelate due to thaw, meltwater, and surface moisture changes.

- **Winter histograms show the strongest right-shifted cases**, especially 2020 P2 and 2021 P2, indicating a larger share of stable coherent scatterers under frozen conditions.
- **However, winter is not always uniformly better**, because some winter pairs are also broad or left-heavy, showing that coherence depends not only on season but also on local surface conditions, snow state, and acquisition timing.

THANK YOU!

Contact:
Marisha Jmukhadze, Author
m.Jmukhadze@gmail.com
Puneeth Bheesetty, Co-investigator
puneeth.bheesetty@gmail.com

References:

- Copernicus Sentinel-1 Mission Data (2019–2024). European Union, Copernicus Programme.
- Torres, R., Snoeij, P., Geudtner, D., Bibby, D., Davidson, M., Attema, E., Potin, P., et al. (2012). *GMES Sentinel-1 mission*. Remote Sensing of Environment, 120, 9–24.
- ESA. (2024). *Sentinel-1 User Guide*. European Space Agency. Available: https://sentinel.esa.int
- ESA. (2024). *SNAP – Sentinel Application Platform Documentation*. European Space Agency. Available: https://step.esa.int
- Hanssen, R. F. (2001). *Radar Interferometry: Data Interpretation and Error Analysis*. Springer.
- Massonnet, D., & Feigl, K. L. (1998). *Radar interferometry and its application to changes in the Earth's surface*. Reviews of Geophysics, 36(4), 441–500.
- Bamler, R., & Hartl, P. (1998). *Synthetic Aperture Radar Interferometry*. Inverse Problems, 14(4), R1–R54.
- Rosen, P. A., Hensley, S., Joughin, I. R., Li, F. K., Madsen, S. N., Rodriguez, E., & Goldstein, R. M. (2000). *Synthetic Aperture Radar Interferometry*. Proceedings of the IEEE, 88(3), 333–382.
- Aslan, G., Rouyet, L., Bredal, M., Lauknes, T. R., Wendt, L., Stødle, D., et al. (2026). *Operational InSAR Monitoring in the High Arctic: The InSAR Svalbard Ground Motion Service*. FRINGE 2026.